



A novel fatty acid-binding protein 5 and 7 inhibitor ameliorates oligodendrocyte injury in multiple sclerosis mouse models

An Cheng^a, Wenbin Jia^a, Ichiro Kawahata^{a,b}, Kohji Fukunaga^{a,b,*}

^a Department of Pharmacology, Graduate School of Pharmaceutical Sciences, Tohoku University, Sendai, Japan

^b Department of CNS Drug Innovation, Graduate School of Pharmaceutical Sciences, Tohoku University, Sendai, Japan

ARTICLE INFO

Article History:

Received 2 June 2021

Revised 27 August 2021

Accepted 3 September 2021

Available online xxx

Keywords:

Multiple sclerosis

Fatty acid-binding proteins

Astrocyte

Microglia

Mitochondria

ABSTRACT

Background: Multiple sclerosis (MS) is an autoimmune disease characterised by the demyelination of mature oligodendrocytes in the central nervous system. Recently, several studies have indicated the vital roles of fatty acid-binding proteins (FABPs) 5 and 7 in regulating the immune response.

Methods: We assessed a novel FABP5/FABP7 inhibitor, FABP ligand 6 (MF 6), as a potential therapeutic for MS therapy. *In vivo*, we established MOG₃₅₋₅₅-administered experimental autoimmune encephalomyelitis (EAE) mice as an MS mouse model, followed by prophylactic and symptomatic treatment with MF 6. The therapeutic effect of MF 6 was determined using behavioural and biochemical analyses. *In vitro*, MF 6 effects on astrocytes and oligodendrocytes were examined using both astrocyte primary culture and KG-1C cell lines.

Findings: Prophylactic and symptomatic MF 6 therapy reduced myelin loss and clinical EAE symptoms. Furthermore, oxidative stress levels and GFAP-positive and ionised calcium-binding adaptor protein-1-positive cells were reduced in the spinal cord of MF 6-treated mice. In addition, MF 6 attenuated lipopolysaccharide-stimulated interleukin-1 β and tumour necrosis factor- α accumulation in primary astrocyte culture. Moreover, MF 6 indicated a powerful protective function for the mitochondria in the oligodendrocytes of EAE mice via FABP5 inhibition.

Interpretations: MF 6 is a potent inhibitor of FABP5 and FABP7; targeted inhibition of the two proteins may confer potential therapeutic effects in MS via immune inhibition and oligodendrocyte protection.

Funding: This work was supported by the Strategic Research Program for Brain Sciences from the Japan Agency for Medical Research and Development (JP17dm0107071, JP18dm0107071, JP19dm0107071, and JP20dm0107071).

© 2021 The Author(s). Published by Elsevier B.V. This is an open access article under the CC BY-NC-ND license (<http://creativecommons.org/licenses/by-nc-nd/4.0/>)

1. Introduction

Multiple sclerosis (MS) is a chronic inflammatory and demyelinating disease that is characterised by multifocal and temporally scattered central nervous system (CNS) damage, manifested as axonal damage [1]. Although autoimmunity plays a major role in the pathogenesis of MS, the precise underlying mechanism remains elusive [2]. The current treatment for MS is divided into three categories: treatment of exacerbations, slowing disease progression with disease-modifying therapies (DMTs), and symptomatic therapies [3]. Among them, DMTs are an integral part of the long-term management of patients with MS, and the goal of disease improvement is to reduce early clinical and subclinical disease activity, which is believed to cause long-term disability [3]. Interferons (IFNs) were the first DMTs approved for MS therapy, of which IFN- β reportedly reduces the

number of exacerbations and suppresses the progression of physical disabilities. However, IFNs are associated with rare allergic reactions, including allergic reactions, seizures, and decreased peripheral blood cell counts. Another DMT available in the market, fingolimod, is a sphingosine-1-phosphate (S1P) agonist that binds and activates S1P receptors. On binding to S1P receptors, fingolimod prevents lymphocytes from exiting the lymph nodes, thus decreasing the number of lymphocytes in peripheral blood and reducing the migration of naïve T cells and memory T cells into the CNS, which in turn impedes the progression of MS [4]. However, treatment with fingolimod is associated with an increased risk of bradyarrhythmia and atrioventricular block [5]. Newer DMTs are more effective than their counterparts; however, several present uncommon but serious potential adverse effects. Thus, there is an urgent need to identify novel targets for MS therapy.

Fatty acid-binding proteins (FABPs) are a family of low molecular weight intracellular proteins with a molecular weight of 14–15 kDa and comprise up to 12 types of molecular species that exhibit distinct

* Corresponding author.

E-mail address: kfukunaga@tohoku.ac.jp (K. Fukunaga).

Research in context

Evidence before this study

Multiple sclerosis (MS) is a potentially disabling disease of the brain and spinal cord (central nervous system) and is characterised by loss of the protective sheath (myelin) that covers nerve fibres, thus resulting in neurotransmission disorders. Several studies have indicated that fatty acid protein 5 (FABP5) and 7 (FABP7) play pivotal roles in pathological progression in an MS mouse model (experimental autoimmune encephalomyelitis [EAE] mice), suggesting novel protein targets for MS therapy.

Added value of this study

We developed a novel ligand (MF 6) exhibiting a high affinity for both FABP5 and FABP7. In EAE mice or primary cultured astrocytes, MF 6 markedly reduced astrocyte- and microglia-dependent inflammatory responses by inhibiting FABP5 and FABP7. Furthermore, in both in vivo and in vitro experiments, MF 6 rescued oligodendrocyte survival by inhibiting mitochondrial macropore formation. Finally, MF 6 reduced the severity of EAE, as assessed by neurological scores in mice. Overall, MF 6 exhibited inhibitory effects that afforded both inflammatory inhibition and oligodendrocyte protection.

Implications of all the available evidence

These findings suggest that MF 6 elicits potent prophylactic and symptomatic effects in EAE mice by inhibiting inflammatory responses and improving oligodendrocyte survival via inhibition of both FABP5 and FABP7. Therefore, MF 6 may represent a novel therapeutic candidate for MS therapy.

transient middle cerebral artery occlusion by inhibiting the expression of FABP5 and FABP7 following brain ischaemia [25].

In the present study, we verified the potential effects of MF 6, a FABP5/FABP7 inhibitor, in MS therapy using a MOG₃₅₋₅₅-generated model of EAE in mice. We observed that MF 6 decreased EAE symptoms following prophylactic and symptomatic treatments, as well as reduced myelin loss and the number of glial fibrillary acidic protein (GFAP)-positive and ionised calcium-binding adaptor protein-1 (Iba-1)-positive cells in the spinal cord. Furthermore, MF 6 blocked interleukin (IL)-1 β and tumour necrosis factor (TNF)- α accumulation in primary astrocyte cultures by inhibiting FABP5 and FABP7. In addition, MF 6 ameliorated mitochondrial injury in oligodendrocytes by blocking FABP5/VDAC-1-induced mitochondrial macropore formation in EAE and KG-1C cells. Overall, the effects of MF 6 on inflammatory inhibition and oligodendrocyte protection in EAE facilitated the therapeutic effects on MS via FABP5 and FABP7 inhibition.

2. Methods

2.1. Animals and EAE induction

Six-week-old female C57BMF/6J mice were obtained from Clea Japan, Inc. (Tokyo, Japan) and maintained in polypropylene cages (temperature: 23 \pm 2°C; humidity: 55 \pm 5%; lights on between 9 a.m. and 9 p.m.). EAE induction was performed in 8–10-week-old female mice. Briefly, mice were injected at two injection sites: the midline of the back just below the shoulders and the lower back. Each site was injected with 50 μ L of emulsion, containing 50 μ g of MOG₃₅₋₅₅ (R&D systems, 149635-73-4) in complete Freund's adjuvant (Sigma-Aldrich, F5881) supplemented with 500 ng of *Mycobacterium tuberculosis* H37Ra (Difco Laboratories, 231141). Additionally, each site was subcutaneously (s.c.) injected with 100 ng of pertussis toxin (List Biological Laboratories, 181) immediately after MOG₃₅₋₅₅ injection, and then again 2 days after immunisation. For the MF 6 treatment group, MF 6 (1 mg/kg) in 200 μ L phosphate-buffered saline (PBS) was administered by intragastric administration (i.g.) 7 days before MOG₃₅₋₅₅ injection (prophylactic treatment) or 12 days after MOG₃₅₋₅₅ injection (symptomatic treatment); treatment was performed daily until four weeks after EAE induction (the spinal cord was fixed on the same day). The EAE group was treated with the same volume of PBS (i.g.). For the control group, mice were treated with PBS (i.g.) only. Clinical scores were designated numerically according to previous reports [26] as follows: 0, no symptoms of disease (asymptomatic); 1, limp tail or hind limb weakness; 2, both limp tail and hind limb weakness; 3, partial paralysis of the hind limbs; 4, complete hind limb paralysis; 5, moribund or dead. For each group, mice were treated and measured randomly, and there were no confounders. For anaesthesia, isoflurane was used during experiment. For euthanasia, mice were injected with overdose of pentobarbital intraperitoneally.

2.2. Primary astrocyte culture

For primary astrocyte culture, P1–2 mouse pups were decapitated, followed by isolation of the cortex from the brain and digestion in a digestion solution (13.6 mL PBS, 0.8 mL DNase I stock solution [0.2 mg/mL], and 0.6 mL of a trypsin stock solution [0.25%]). The tissue was then sliced using a sterilised razor blade into approximately 1 mm³ chunks, centrifuged at 100 \times g for 5 min, and resuspended in DMEM20S medium (DMEM, 4 mM L-glutamine, 1 mM sodium pyruvate, 20% foetal bovine serum [FBS], 50 U/mL penicillin, and 50 μ g/mL streptomycin). The tissue suspension was strained using a 70 μ m nylon cell strainer, seeded in poly L-lysine-coated tissue culture flasks and cultured in DMEM20S medium for 2 weeks (mixed culture). The flasks were shaken for 24 h at 200 rpm at 37°C to remove microglial cells and oligodendrocytes, and the residual cells were considered crude astrocyte cultures. Finally, astrocytes were stained with GFAP.

tissue specificity [6]. Among them, the heart-type (FABP3), brain-type (FABP7), and epidermal-type (FABP5) are expressed in the brain. In addition to their original function as a lipid chaperone in regulating the uptake and transportation of long-chain fatty acids, [7,8] FABPs are reportedly involved in neuronal injury and inflammatory pathways [9,10] in various neurodegenerative diseases [11–14]. Notably, FABP5 deficiency afforded protection against experimental autoimmune encephalomyelitis (EAE), a well-established mouse model of MS [15,16]. FABP5-deficient dendritic cells reportedly exhibit decreased production of proinflammatory cytokines, thereby down-regulating Th1 and Th17 responses [16]. In addition, FABP5 inhibition via suppression of peroxisome proliferator-activated receptor (PPAR) γ expression decreased T cell differentiation, thereby reducing the clinical symptoms of EAE [17]. Moreover, glial cells in the CNS, such as microglia, astrocytes, and oligodendrocytes, play a vital role in mediating various aspects of MS [18,19]. Kamizato et al. have demonstrated that FABP7 inhibits the induction of inflammation, which leads to demyelination through spinal cord astrocyte function in the early phase of EAE [21]. However, FABP7 deficiency significantly reduced the clinical score of EAE in mice [20]. Accordingly, inhibition of FABP5 and FABP7 may be a potential target for MS therapy.

In previous studies, FABP ligand 6 (MF 6) has exhibited a high binding affinity for FABP5 ($K_D=874\pm66$ nM) [21] and FABP7 ($K_D=20\pm9$ nM) [22], but not for FABP3 ($K_D=1038\pm155$ nM) [23]. *In vitro*, MF 6 was shown to rescue mitochondrial function by blocking voltage-dependent anion channel (VDAC)-1-dependent mitochondrial macropore formation induced by psychosine in KG-1C cells, a FABP5-mediated injury [24]. Previously, we have reported that MF 6 binds to the lipid-binding site of FABP7 and inhibits FABP7-induced alpha-synuclein toxicity in glial cells and oligodendrocytes [22]. MF 6 also significantly rescued ischaemia-reperfusion injury in mice with

2.3. Cell culture

KG-1C human oligodendroglial cells (RRID: CVCL_2971) were obtained from the RIKEN BRC Cell Bank (Tsukuba, Japan). Short-tandem repeat (STR) profiling of cell lines was performed by JCRB. Cells were cultured in Dulbecco's Modified Eagle Medium (DMEM) with 10% FBS and penicillin/streptomycin (100 U/100 μ g/mL) at 37°C under 5% CO₂. Lysophosphatidylcholine (LPC) was dissolved in methanol and stored at -30°C until use.

2.4. Protein extraction

Culture cells or isolated spinal cords were frozen in liquid nitrogen and stored at -80°C until use. Samples were homogenised with 50 μ L (for each 35 mm dish) or 200 μ L (for spinal cords) of Triton X-100 buffer containing 0.5% Triton X-100 at pH 7.4, 4 mM ethylene glycol, 50 mM Tris-HCl, 10 mM ethylenediaminetetraacetic acid, 1 mM sodium orthovanadate, 50 mM sodium fluoride, 40 mM Na₄P₂O₇·10H₂O, 0.15 M sodium chloride, 50 μ g/mL leupeptin, 25 μ g/mL pepstatin A, 50 μ g/mL trypsin inhibitor, 100 nM calyculin A, and 1 mM dithiothreitol. The concentration of the supernatant protein was normalised using the Bradford assay.

2.5. Mitochondria isolation

Mitochondria were isolated as described previously [24]. In brief, spinal cords or collected cells were suspended using mitochondrial isolation buffer (250 mM sucrose, 1 mM dithiothreitol, 10 mM KCl, 1 mM ethylenediaminetetraacetic acid, 1.5 mM MgCl₂, protease inhibitors, and 20 mM Tris-HCl, pH 7.4), homogenised with a glass homogeniser at approximately 50 strokes per pestle, and centrifuged three times at 800 \times g for 10 min. The supernatant proteins were collected and centrifuged at 15,000 \times g for 10 min at 4°C. Supernatants were collected as cytosolic fractions (without mitochondria). The mitochondrial pellets were immediately washed three times with mitochondrial isolation buffer and homogenised with Triton X-100 buffer. The supernatant proteins were collected as mitochondrial fractions. Protein concentrations of isolated mitochondria were normalised using the Bradford assay. The number of mitochondria was estimated using VDAC-1 using western blotting (WB).

2.6. Immunoblotting analysis

Extracts from spinal cords, cells, or isolated mitochondria were separated by sodium dodecyl sulphate-polyacrylamide gel electrophoresis (SDS-PAGE) using a commercially available gel (Cosmo Bio Co., Ltd.) and then transferred to poly(vinylidene fluoride) (PVDF) membranes. The membranes were incubated with primary antibodies against caveolin-1, Iba-1, 4-hydroxynonenal (4-HNE), TNF- α , IL-1 β , myelin basic protein (MBP), FABP5, FABP7, VDAC-1, β -tubulin, dsDNA, and cytochrome C, followed by treatment with a horseradish peroxidase (HRP)-conjugated secondary antibody (anti-mouse IgG [H&L], anti-rabbit IgG [H&L], and anti-goat IgG [H&L]), and detected with an ECL detection system (Amersham Biosciences, NJ, USA) using the Image Quant LAS 4000 mini system. Intensity quantification was conducted using Image Gauge software (version 3.41; Fuji Film, Tokyo, Japan).

2.7. Immunoprecipitation analysis

For immunoprecipitation analysis, 100 μ L of protein A-Sepharose CL-4B (50%, v/v) was suspended in PBS in a total volume of 1000 μ L and stored at 4°C. Spinal cord extracts containing 500 μ g of protein were incubated for 4 h at 4°C with 10 μ g of anti-FABP5 antibody and 5 μ g of anti-VDAC-1 antibody. The mixture was incubated

overnight at 4°C. The samples were then separated using SDS-PAGE using a commercially available gel (Cosmo Bio Co., Ltd.).

2.8. Dot blot assay

A dot blot assay was performed to determine dsDNA levels in the mitochondrial fraction as previously described [27]. In brief, a PVDF membrane (Millipore) was placed on the top of the soaked sheets, and equal amounts of protein in a similar volume were placed in dots in specific zones. After the dots dried, the membrane was blocked with 5% nonfat milk in TTBS buffer (0.1% Tween 20 in Tris-buffered saline) for 1 h at room temperature. Membranes were subjected to WB as described above (primary antibodies against dsDNA and VDAC-1), followed by treatment with an HRP-conjugated secondary antibody (anti-mouse IgG H&L and anti-rabbit IgG H&L).

2.9. Immunofluorescence staining and confocal microscopy

Immunofluorescence staining was performed as previously described [28]. In the present study, cells were incubated with primary antibodies against 4-HNE, Iba-1, Olig2, NeuN, GFAP, FABP5, FABP7, and TOM20. Fluorescein, Alexa 405-labelled anti-mouse IgG, Alexa 488-labelled anti-goat IgG, Alexa 594-labelled anti-mouse IgG, and Alexa 594-labelled anti-rabbit IgG were used for detection. Mito-Tracker (CST) and Alexa Fluor™ 488 Phalloidin (Thermo Fisher Scientific) were used for mitochondria and filamentous actin staining, respectively. Immunofluorescent images were analysed using a confocal laser scanning microscope (DMi8; Leica, Wetzlar, Germany).

2.10. FABP5/7 shRNA plasmid and shRNA delivery

Human-FABP5 shRNA bacterial stock was obtained from Sigma-Aldrich, and the sequences were as follows: shRNA1 (CCGGTGGAGTGTGTCATGAACAATCTCGAGATTGTCATGACACACTCCACTTTTTTG), shRNA2 (CCGGCAACTTTACAGATGGTGCATCTCGA-GATGCACCATCTGTAAAGTTGCTTTTTG), and shRNA3 (CCGGT GAGCAAATCTCCATACTGTTCCGAGAACAGTATGGAGATTTGC TCATT TTTTG). Human-FABP7 shRNA bacterial stock was obtained from Sigma-Aldrich, and the sequences were as follows: shRNA1 (CCGGCATA CAGAAATGGGATGGCAACTCGAGTTGCCATCCCATTCTGTATGTTTTTG), shRNA2 (CCG GGGTTGCTGTTCCCACTATGACTCGAGT-CATAGTGGCGAACAGCAACCTTTTTTG), and shRNA3 (CCGACAACAT GGCTGATCATTAATCTCGAGATTAATGATCAGCCATGTTGTTTT TTTG). The plasmid was purified using the GenElute™ HP Plasmid Maxiprep Kit (Sigma, St. Louis, MO, USA). Primary astrocytes were transduced with an empty vector or shRNA plasmid (2 μ g per 35-mm dish) using Lipofectamine LTX and Plus Reagent (Invitrogen, Carlsbad, CA, USA) and Opti-MEM (Thermo Fisher Scientific, Waltham, MA, USA), according to the manufacturer's protocol.

2.11. Cell death assay

Cell viability was measured using a cell counting kit (Dojindo) according to the manufacturer's instructions. The absorbance of the viable cells was measured at a test wavelength of 400 nm and a reference wavelength of 450 nm using a FlexStation 3 Multi-Mode Microplate Reader (Molecular Devices, San Jose, CA, USA).

2.12. JC-1 assay

Mitochondrial membrane potential was measured using the JC-1 Mito MP Detection Kit (Dojindo). In brief, the culture cells were washed with PBS and stained according to the manufacturer's instructions. The relative degrees of mitochondrial polarisation were quantified by measuring the red-shifted JC-1 aggregates at 535 nm (Ex) and 585-605 nm (Em) and green-shifted JC-1 aggregates at 485

nm (Ex) and 525–545 nm (Em) using a FlexStation 3 Multi-Mode Microplate Reader (Molecular Devices, San Jose, CA, USA).

2.13. MF 6

MF 6 was synthesised by Shiratori Pharmaceutical Co., Ltd. Additional details are provided in the Supplementary Material section.

2.14. Statistics

Data were analysed using GraphPad Prism 7 (GraphPad Software, Inc., La Jolla, CA, USA) and are expressed as the mean \pm standard error of the mean (SEM). The normality assumption was examined using the Shapiro-Wilk test, and the equal variance assumption was examined by the Brown-Forsythe test using GraphPad Prism 7. For the data that passed these assumptions, significant differences were determined using Student's *t*-test for two-group comparisons (Fig. 1e; Fig. 2c; Fig. 5h, i) and by one-way analysis of variance (ANOVA) for other multigroup comparisons, followed by Tukey's multiple comparisons test. For data that did not pass these assumptions, the significant differences were determined using the Kruskal-Wallis test (nonparametric version of ANOVA) (Fig. 1k, n; Fig. 2g, k; Fig. 3c, g; Fig. 5r). Statistical significance was set at $p < 0.05$.

2.15. Ethics statement

All animal experiments were reviewed and approved by the Institutional Animal Care and Use Committee of the Tohoku University Environmental and Safety Committee (2019PhLM0-021 and 2019PhA-024). All animal experiments were performed following the animal use guidelines and ethical approval.

2.16. Role of funder

The funders were not involved in the study design, data collection, analysis, interpretation, decision to publish, or writing of the manuscript. The writing group (including the corresponding author) had full access to all the data in the study and had final responsibility for the decision to submit the manuscript for publication.

3. Results

3.1. MF 6 attenuates EAE symptoms both prophylactic and symptomatic treatments in vivo

In previous studies, FABP5 and FABP7 deficiency conferred protective effects against EAE development, [17,20] suggesting an important role of FABP5 and FABP7 in EAE progression. Herein, we evaluated the therapeutic efficacy of MF 6 (Fig. 1a), which has a high affinity for both FABP5 and FABP7, using a mouse model of EAE (Fig. 1b) [26]. EAE mice were orally administered MF 6 (1 mg/kg), which is the maximum effective dose in brain ischemia [25] 1 week before MOG immunisation of the EAE model (Fig. 1c). MF 6 administration significantly reduced the severity of EAE, as assessed by the area under the curve (AUC) of clinical scores (EAE group: 42.21 ± 4.675 ; EAE + MF 6 group: 17.88 ± 4.08 ; $p < 0.01$, vs. EAE group; $F(5, 5) = 1.31$, $n = 6$) (Fig. 1d, e). As caveolin-1, Iba-1, TNF- α , and IL-1 β are widely used as inflammation markers, and 4-HNE is an oxidative stress marker, we analysed the levels of these factors using WB to further determine whether MF6 improves inflammation and oxidative injury in EAE mice (Fig. 1f). Our results revealed reduced inflammatory and oxidative levels, along with decreased levels of caveolin-1 (EAE group: 4.10 ± 0.39 ; EAE + MF 6 group: 2.28 ± 0.32 ; $p < 0.01$, vs. EAE group; $F(2, 9) = 28.14$, $n = 4$) (Fig. 1g), Iba-1 (EAE group: 1.91 ± 0.11 ; EAE + MF 6 group: 1.39 ± 0.10 ; $p < 0.01$, vs. EAE group; $F(2, 9) = 26.22$, $n = 4$) (Fig. 1h), 4-HNE (EAE group: 3.76 ± 0.33 ; EAE + MF

6 group: 2.07 ± 0.3488 ; $p < 0.01$, vs. EAE group; $F(2, 9) = 23.17$, $n = 4$) (Fig. 1i), IL-1 β (EAE group: 2.05 ± 0.23 ; EAE + MF 6 group: 1.11 ± 0.12 ; $p < 0.01$, vs. EAE group; $F(2, 9) = 14.20$, $n = 4$) (Fig. 1j), and TNF- α (EAE group: 2.04 ± 0.20 ; EAE + MF 6 group: 1.018 ± 0.14 ; $p = 0.0558$, vs. EAE group; $n = 4$) (Fig. 1k) in MF 6-treated mice as shown by WB. In addition, the levels of MBP were upregulated in the MF6 group (EAE group: 0.34 ± 0.02 ; EAE + MF 6 group: 0.71 ± 0.05 ; $p < 0.01$, vs. EAE group; $F(2, 9) = 57.54$, $n = 4$) (Fig. 1l). However, WB revealed no significant changes in the levels of FABP5 and FABP7 in both the EAE models and the MF 6-treated mice when compared with the levels of β -tubulin (Fig. 1f). Significant changes in FABP5 levels (EAE group: 3.53 ± 0.42 ; EAE + MF 6 group: 1.49 ± 0.18 ; $p < 0.01$, vs. EAE group; $F(2, 9) = 24.49$, $n = 4$) (Fig. 1m) and an obvious but not significant decrease in FABP7 levels (EAE group: 3.06 ± 0.76 ; EAE + MF 6 group: 0.95 ± 0.18 ; $p = 0.0723$, vs. EAE group; $n = 4$) (Fig. 1n) were apparent, compared with the levels of MBP.

As MS therapy is typically initiated after the disease has been active and diagnosed, we further investigated whether MF 6 administration was effective for treating active EAE. Accordingly, we treated EAE mice with MF 6 along with MOG immunisation on day 12 (Fig. 2a). Consistently, MF 6 significantly reduced the severity of EAE, as assessed by the AUC of the clinical scores (EAE group: 42.72 ± 2.56 ; EAE + MF 6 group: 24.54 ± 1.61 ; $p < 0.01$, vs. EAE group; $F(7, 6) = 2.90$, $n = 7$) (Fig. 2c). In addition, in symptomatic treatment cases (Fig. 2d), MF 6 showed a possibly potent effect in decreasing the upregulated levels of caveolin-1 (EAE group: 4.573 ± 0.55 ; EAE + MF 6 group: 2.234 ± 0.25 ; $p < 0.01$, vs. EAE group; $F(2, 11) = 23.03$, $n = 5$) (Fig. 2e), Iba-1 (EAE group: 3.771 ± 0.53 ; EAE + MF 6 group: 2.06 ± 0.26 ; $p < 0.05$, vs. EAE group; $F(2, 11) = 13.72$, $n = 5$) (Fig. 2f), 4-HNE (EAE group: 2.34 ± 0.34 ; EAE + MF 6 group: 1.39 ± 0.24 ; $p = 0.35$, vs. EAE group; $F(2, 11) = 7.16$, $n = 5$) (Fig. 2g), IL-1 β (EAE group: 2.58 ± 0.31 ; EAE + MF 6 group: 1.72 ± 0.13 ; $p < 0.05$, vs. EAE group; $F(2, 11) = 11.56$, $n = 5$) (Fig. 2h), and TNF- α (EAE group: 2.71 ± 0.15 ; EAE + MF 6 group: 1.36 ± 0.17 ; $p < 0.05$, vs. EAE group; $F(2, 11) = 38.59$, $n = 5$) (Fig. 2i) in EAE mice. Furthermore, MF 6 group exhibited higher MBP levels when compared with those detected in EAE mice (EAE group: 0.59 ± 0.06 ; EAE + MF 6 group: 1.01 ± 0.06 ; $p < 0.01$, vs. EAE group; $F(2, 17) = 19.67$, $n = 5$) (Fig. 2j). Consistent with the prophylactic treatment findings, symptomatic treatment with MF 6 significantly decreased both FABP5 (EAE group: 1.76 ± 0.11 ; EAE + MF 6 group: 1.17 ± 0.13 ; $p < 0.05$, vs. EAE group; $n = 5$) (Fig. 2k) and FABP7 (EAE group: 1.48 ± 0.12 ; EAE + MF 6 group: 0.90 ± 0.10 ; $p < 0.05$, vs. EAE group; $F(2, 11) = 7.41$, $n = 5$) (Fig. 2l) levels when compared with MBP levels.

Collectively, our findings indicated that MF 6 is a potent ligand that attenuates EAE clinical symptoms by decreasing inflammatory and oxidative levels in the spinal cord, as well as by protecting oligodendrocytes.

3.2. MF 6 decreases oxidative stress levels in the spinal cord

Similar to previous reports, [29,30] we investigated the relationship between oxidative stress levels and spinal cord injury in EAE mice. To verify the oxidative levels in different cell types, we co-immunostained spinal cord slices (Fig. 3a) with the oxidative marker 4-HNE and markers of microglia (Iba-1), oligodendrocytes (Olig2), and neurons (NeuN). As expected, we detected an elevated number of 4-HNE-positive cells in the white matter and grey matter of the spinal cord in EAE mice when compared with that in control mice (4-HNE-positive cells in the control group: 5.20 ± 1.04 ; EAE group: 42.14 ± 3.35 ; $p < 0.01$, vs. control group; $n = 7$) (Fig. 3b, c). Surprisingly, MF 6 almost completely suppressed the upregulated oxidative stress levels and significantly decreased the number of 4-HNE-positive cells (4-HNE-positive cells in EAE + MF 6 group: 9.0 ± 1.38 ; $p < 0.05$, vs. EAE group; $n = 10$) (Fig. 3c). Additionally, on co-staining slices with 4-HNE and Iba-1 (microglia marker), no double-positive

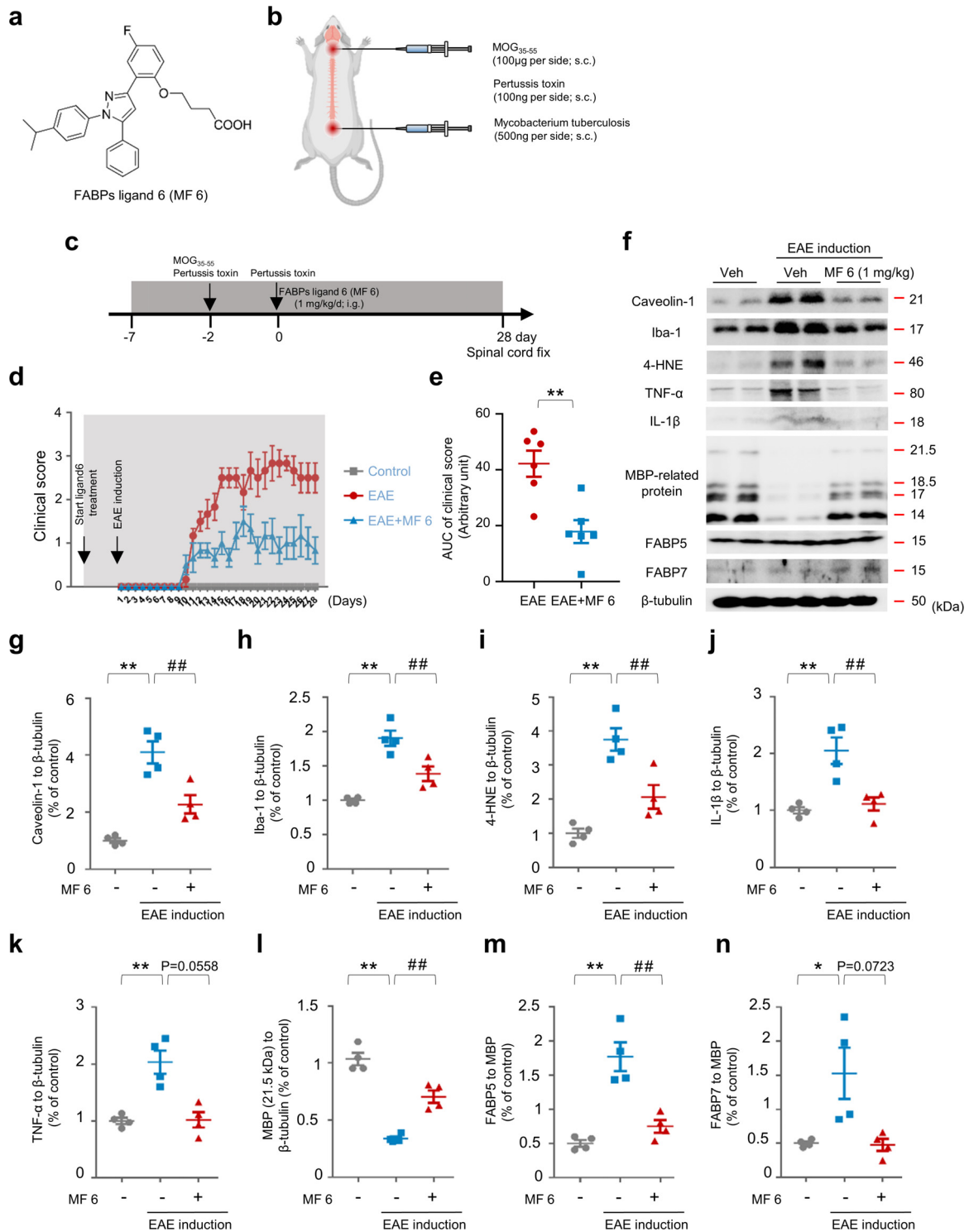


Fig. 1. Prophylactic treatment with MF 6 attenuates clinical symptoms of EAE. (a) Chemical structure of MF 6. (b) Schematic diagram of EAE induction; female C57BMF/6J mice were injected with MOG₃₅₋₅₅ at two injection sites. (c) Protocol for EAE induction and MF 6 prophylactic treatment. (d) Quantification of clinical scores. EAE-induced C57BMF/6J mice were treated with MF 6 (1 mg/kg) (n=6) or PBS (n=6) vehicle and were scored daily after immunisation. (e) Quantification of the area under the curve (AUC) of clinical scores (n=6). (f) Immunoblots and densitometry of the spinal cord of EAE mice treated with MF 6 or PBS vehicle and against caveolin-1, Iba-1, 4-HNE, IL-1β, TNF-α, MBP, FABP5, FABP7, and β-tubulin. (g-n) Quantification of (f) (n=4), showing that prophylactic treatment with MF 6 significantly decreases levels of caveolin-1, Iba-1, 4-HNE, IL-1β, and TNF-α and increases levels of MBP protein, as well as reduces levels of FABP5 and FABP7 when compared with MBP. Data are shown as mean ± standard error of the mean (SEM) and were obtained using student's *t*-test, one-way ANOVA, or Kruskal-Wallis test. **p*<0.05, ***p*<0.01, and ****p*<0.01. EAE, experimental autoimmune encephalomyelitis; PBS, phosphate-buffered saline; s.c., subcutaneously; i.g., intragastric administration; Veh., vehicle; Iba-1, ionised calcium-binding adaptor protein-1; 4-HNE, 4-hydroxynonenal; IL-1β, interleukin-1β; TNF-α, tumour necrosis factor-α; MBP, myelin basic protein; FABP5, fatty acid protein 5; FABP7, fatty acid protein 7.

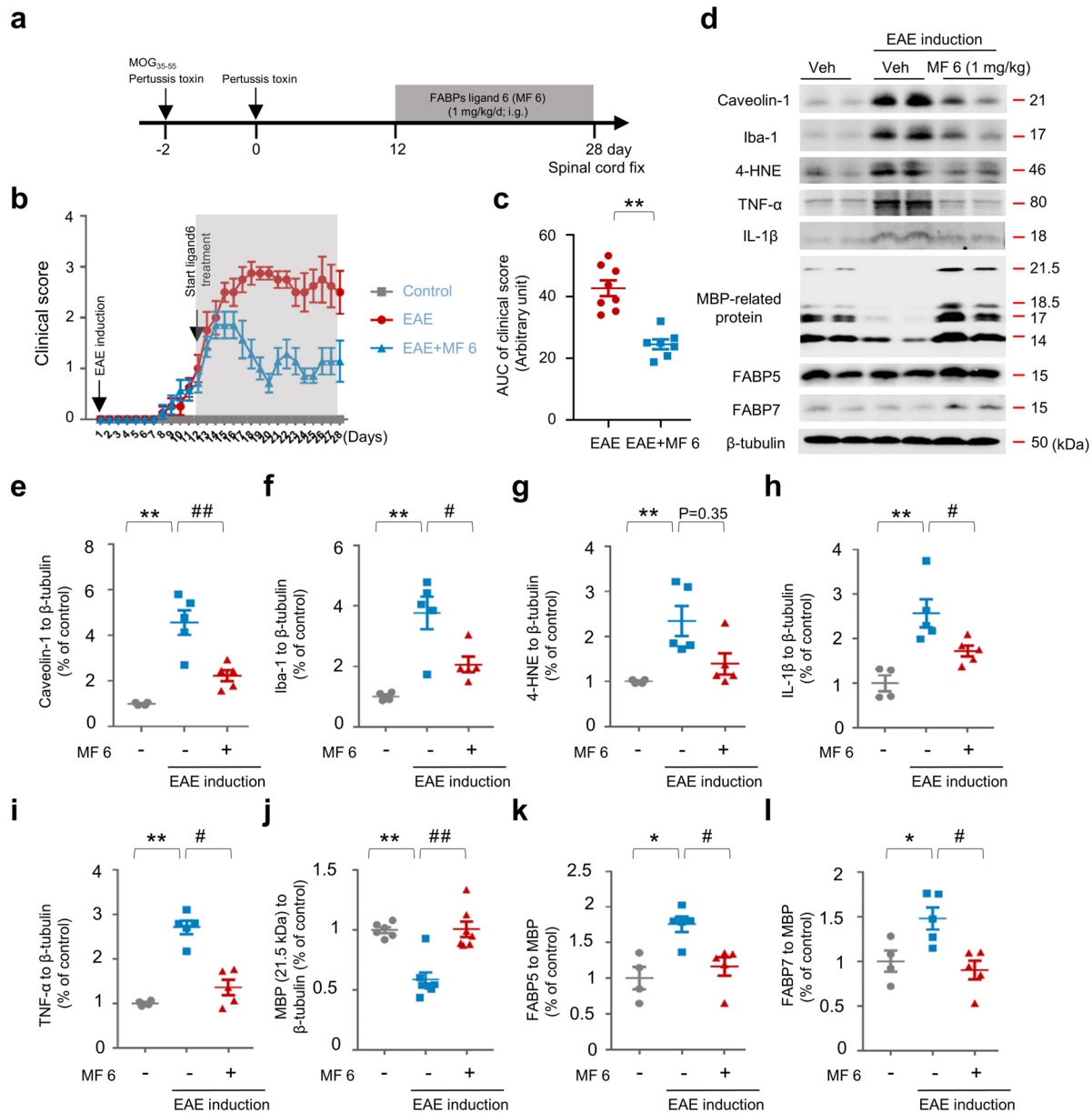


Fig. 2. Symptomatic treatment with MF 6 attenuates clinical symptoms of EAE. (a) Protocol of EAE induction and MF 6 symptomatic treatment. (b) Quantification of clinical scores. EAE-induced C57BMF/6J mice were treated with MF 6 (1 mg/kg) (n=7) or PBS (n=7) vehicle and were scored daily after immunisation. (c) Quantification of the area under the curve (AUC) of clinical scores (n>7). (d) Immunoblots and densitometry of the spinal cord of EAE mice treated with MF 6 or PBS vehicle and against caveolin-1, Iba-1, 4-HNE, IL-1 β , TNF- α , MBP, FABP5, FABP7, and β -tubulin. (e-l) Quantification of (d) (n>4), showing that symptomatic treatment with MF 6 significantly decreases levels of caveolin-1, Iba-1, 4-HNE, IL-1 β , and TNF- α and increases levels of MBP-related protein, as well as reduces levels of FABP5 and FABP7 when compared with MBP. Data are shown as mean \pm standard error of the mean (SEM) and were obtained using a one-way ANOVA or Kruskal-Wallis test. * p <0.05, ** p <0.01, # p <0.05 and ## p <0.01. EAE, experimental autoimmune encephalomyelitis; PBS, phosphate-buffered saline; i.g., intragastric administration; Veh., vehicle; Iba-1, ionised calcium-binding adaptor protein-1; 4-HNE, 4-hydroxynonenal; IL-1 β , interleukin-1 β ; TNF- α , tumour necrosis factor- α ; MBP, myelin basic protein; FABP5, fatty acid protein 5; FABP7, fatty acid protein 7.

cells were detected in the spinal cord of EAE mice, although the number of Iba-1-positive cells increased by approximately six-fold when compared with that in control mice (Iba-1-positive cells in the control group: 5.7 ± 1.24 ; EAE group: 26.54 ± 1.99 ; $p < 0.01$, vs. control group; $n = 13$) (Fig. 3d), indicating the upregulation of microglial migration. This result differs slightly from that reported in our previous study, in which the number of 4-HNE/Iba-1-positive cells significantly increased in the hippocampus of olfactory bulbectomised mice [31]. In addition, MF 6 treatment significantly decreased the number of Iba-1-positive cells (Iba-1-positive cells in EAE + MF 6 group: 16.80 ± 1.45 ; $p < 0.01$, vs. EAE group; $F(2, 30) = 38.93$, $n = 10$) (Fig. 3d), indicating attenuated inflammatory levels.

Furthermore, it is crucial to determine the response of oligodendrocytes to immune inflammation, which is directly related to

demyelination. In the present study, we performed co-staining with 4-HNE with Olig2. As expected, in EAE mice, the number of 4-HNE/Olig2-positive cells increased by approximately seven-fold in the white matter (4-HNE/Olig2-positive cells in the control group: 1.60 ± 0.43 ; EAE group: 13.75 ± 1.58 ; $p < 0.01$, vs. control group; $n = 8$) (Fig. 3e, g). Thus, the upregulated oxidative stress levels can be considered the main factor responsible for the death of oligodendrocytes and myelin loss in the spinal cord of EAE mice [32]. Importantly, MF 6 treatment markedly attenuated oxidative stress levels in oligodendrocytes and reduced the number of 4-HNE/Olig2 double-positive cells (4-HNE/Olig2-positive cells in the EAE + MF 6 group: 3.60 ± 0.70 ; $p < 0.05$, vs. EAE group; $n = 10$) (Fig. 3g). Furthermore, to understand whether immune inflammation affects neurons in the grey matter of the spinal cord, we performed co-staining with NeuN with

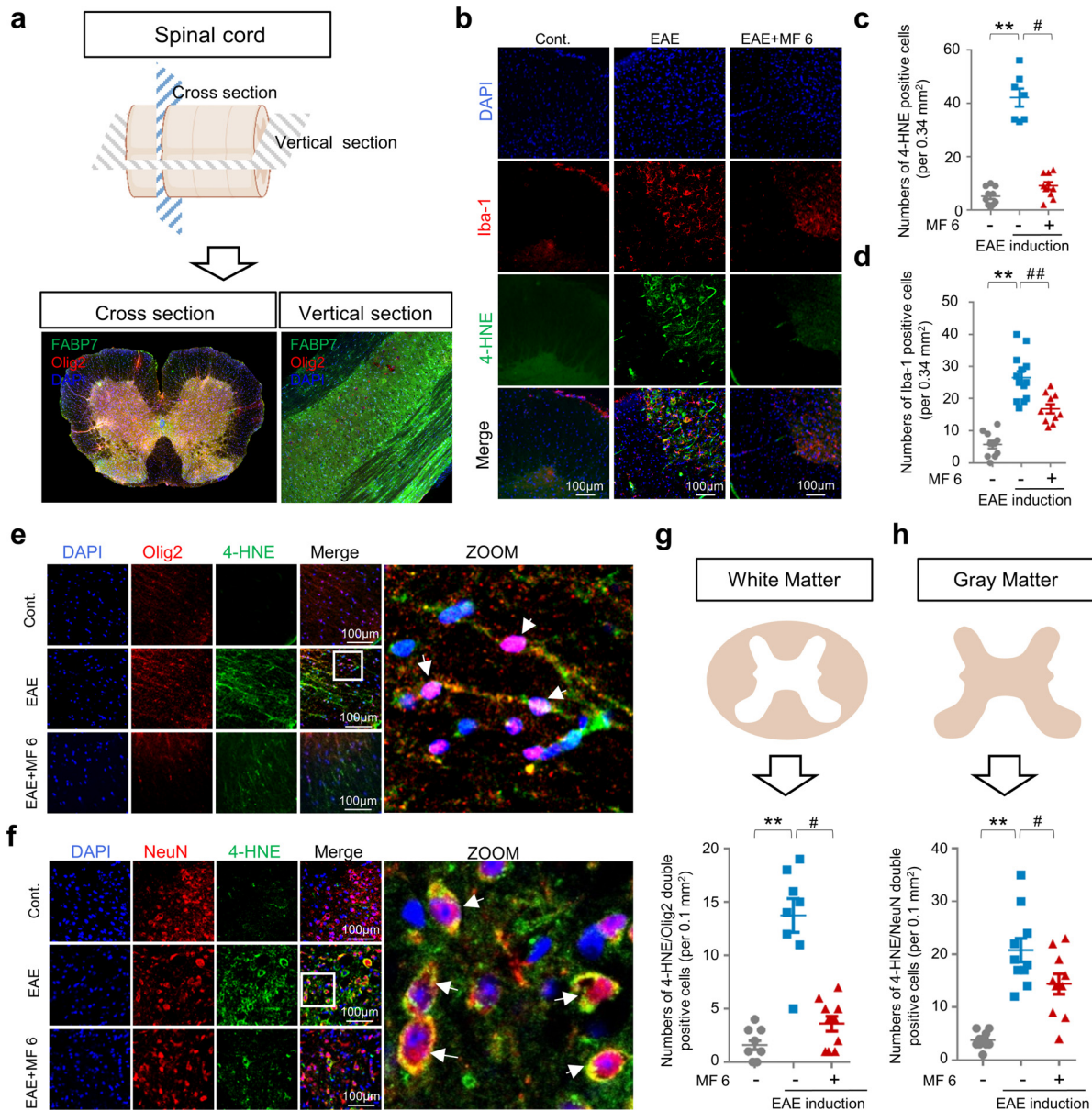


Fig. 3. Symptomatic treatment with MF 6 attenuates oxidative stress levels in the spinal cord. (a) Top, schematic diagram of spinal cord section; bottom, confocal microscopy of immunofluorescence staining of FABP7 (green), Olig2 (red), and DAPI (blue) in a cross-section and vertical section of the spinal cord, respectively. (b) Confocal microscopy of immunofluorescence staining of Iba-1 (red) and 4-HNE (green), revealing that symptomatic treatment with MF 6 (1 mg/kg) decreases microglial migration and oxidative levels in the spinal cord. (c and d) Quantification of (b), 4-HNE-positive cells ($n > 7$) (c) and Iba-1-positive cells ($n > 10$) (d), respectively. (e) Confocal microscopy of immunofluorescence staining of Olig2 (red) and 4-HNE (green), showing that symptomatic treatment with MF 6 (1 mg/kg) reduces oxidative levels in the oligodendrocytes in the white matter of the spinal cord. (f) Confocal microscopy of immunofluorescence staining with NeuN (red) and 4-HNE (green) following symptomatic treatment with MF 6 (1 mg/kg). MF 6 decreases oxidative levels in the neurons of the grey matter in the spinal cord. (g) Top, schematic diagram of the white matter; bottom, quantification of (e) ($n > 8$). (h) Top, schematic diagram of the grey matter; bottom, quantification of (f) ($n = 10$). Data are shown as mean \pm standard error of the mean (SEM) and were obtained using a one-way ANOVA or Kruskal-Wallis test. ** $p < 0.01$, # $p < 0.05$, and ## $p < 0.01$. Cont., control; EAE, experimental autoimmune encephalomyelitis; Iba-1, ionised calcium-binding adaptor protein-1; 4-HNE, 4-hydroxynonenal; FABP7, fatty acid protein 7.

4-HNE. We detected an increased number of 4-HNE/NeuN double-positive cells (4-HNE/NeuN-positive cells in the control group: 3.89 ± 0.49 ; EAE group: 20.80 ± 2.27 ; $p < 0.01$, vs. control group; $n = 10$) (Fig. 3f, h), suggesting oxidative neuronal injury in EAE mice. However, MF 6 had a lower impact on the reduction of oxidative stress in neurons than in oligodendrocytes (4-HNE/NeuN-positive cells in the EAE + MF 6 group: 14.40 ± 1.93 ; $p < 0.05$, vs. EAE group; $F(2, 27) = 24.34$, $n = 10$) (Fig. 3h); this finding could be explained by the fact that FABP5 and FABP7 are not endogenously expressed in neurons, and MF 6, which targets FABP5 and FABP7, cannot function directly in neurons.

Overall, oxidative stress was significantly elevated, especially in the oligodendrocytes and neurons in the spinal cord of EAE mice, and

MF 6 treatment almost completely blocked oxidative stress accumulation, especially in oligodendrocytes, but had a less effect on neurons.

3.3. MF 6 inhibits astrocyte activation

It has been previously established that EAE is mediated by the myelin-reactive T cell response against mature oligodendrocytes and possesses an inflammatory signature [33,34]. In the CNS, microglia and astrocytes are also involved in the EAE inflammatory response, [19,35] in addition to IL- β and TNF accumulation [36]. Previous studies have shown that FABP5 inhibition mediated by inhibitors significantly suppresses lymphocyte migration and pathogenic functions

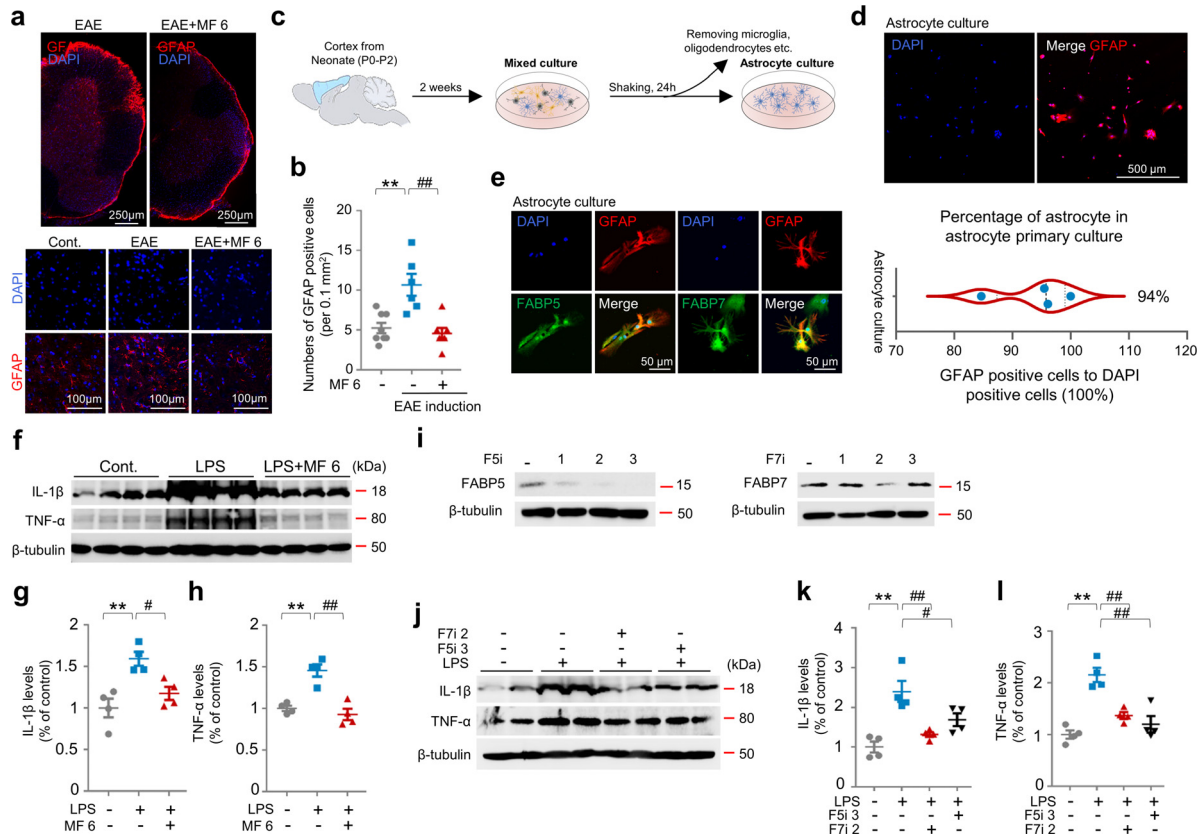


Fig. 4. MF 6 attenuates the activated astrocyte-related inflammatory response. (a) Confocal microscopy of immunofluorescent GFAP-stained sections (red). (b) Quantification of (a); symptomatic treatment with MF 6 (1 mg/kg) ($n > 6$) significantly decreases the number of GFAP-positive cells in the spinal cord. (c) Schematic diagram of astrocyte primary culture from the cortex of P1-2 mouse pups. (d) Top, confocal microscopy of immunofluorescent GFAP (red) and DAPI (blue) staining of primary astrocytes; bottom, quantification of astrocyte purity (GFAP-positive cells to DAPI positive cells) ($n = 4$). (e) Confocal microscopy of immunofluorescent GFAP (red) and FABP5 or FABP7 (green) staining of primary astrocytes. (f) Immunoblots and densitometry of astrocytes against antibody IL-1 β , TNF- α , and β -tubulin. Primary astrocytes were treated with LPS (10 μ g/mL) for 48 h to simulate inflammatory response, and MF 6 (1 μ M) treatment was simultaneously performed. (g and h) Quantification of (e); MF 6 significantly decreases IL-1 β ($n = 4$) and TNF- α ($n = 4$) accumulation in primary astrocytes. (i) Immunoblots and densitometry of astrocytes transfected with FABP5 shRNA (left) and FABP7 shRNA (right), revealing that F5i 3 and F7i 2 are the most efficient. (j) Immunoblots and densitometry of astrocytes against antibody IL-1 β , TNF- α , and β -tubulin; primary astrocytes were stimulated with LPS and knocked down with FABP5 and FABP7. (k and l) Quantification of (j); knockdown of FABP5 and FABP7 significantly decreases IL-1 β and TNF- α levels in primary astrocytes ($n = 4$). Data are shown as mean \pm standard error of the mean (SEM) and were obtained using a one-way ANOVA. ** $p < 0.01$, # $p < 0.05$, and ## $p < 0.01$. Cont., control; EAE, experimental autoimmune encephalomyelitis; GFAP, glial fibrillary acidic protein; FABP5, fatty acid protein 5; FABP7, fatty acid protein 7; IL-1 β , interleukin-1 β ; TNF- α , tumour necrosis factor- α ; LPS, lipopolysaccharide.

via T cell regulation [17]. Herein, we mainly focused on assessing whether inhibition of FABP5 or FABP7 also plays a role in regulating astrocyte-dependent inflammatory responses. The number of GFAP-positive cells increased by approximately two-fold in the spinal cord of EAE mice (GFAP-positive cells in control group: 5.25 ± 0.65 ; EAE group: 10.67 ± 1.38 ; $p < 0.01$, vs. control group; $n = 6$) (Fig. 4a, b); MF 6 significantly suppressed the abnormal increase in GFAP-positive cells (GFAP-positive cells in EAE + MF 6 group: 4.57 ± 0.69 ; $p < 0.01$, vs. EAE group; $F(2, 18) = 12.76$, $n = 7$) (Fig. 4b). Furthermore, to determine whether MF 6 also impacts the levels of proinflammatory cytokines such as TNF- α and IL-1 β , we cultured astrocytes (Fig. 4c), and the purity of astrocytes was approximately 94% ($94 \pm 3.29\%$, $n = 4$) (Fig. 4d). Meanwhile, we observed that primary astrocytes endogenously expressed both FABP5 and FABP7 (Fig. 4e). To trigger the cellular inflammatory response, we treated astrocytes with lipopolysaccharide (LPS; 10 μ g/mL) for 48 h and observed significant accumulation of both IL-1 β (control group: 1.00 ± 0.11 ; EAE group: 1.59 ± 0.08 ; $p < 0.01$, vs. control group; $n = 4$) (Fig. 4f, g) and TNF- α (control group: 1.00 ± 0.03 ; EAE group: 1.46 ± 0.07 ; $p < 0.01$, vs. control group; $n = 4$) (Fig. 4f, h) in LPS-treated cells. As expected, in the MF 6-treated astrocytes, we observed significantly attenuated IL-1 β (EAE + MF 6 group: 1.18 ± 0.08 ; $p < 0.05$, vs. EAE group; $F(2, 9) = 10.73$, $n = 4$) (Fig. 4g) and TNF- α (EAE + MF 6 group: 0.93 ± 0.07 ; $p < 0.01$, vs. EAE group; $F(2, 9) = 21.93$, $n = 4$) (Fig. 4h) levels, indicating a suppressed inflammatory response. However, the FABP

inhibitor MF 6 has a high affinity for both FABP5²¹ and FABP7. This binding and regulation mediated by MF 6 attenuated the inflammatory response in activated astrocytes. To bridge this gap, we knocked down FABP5 and FABP7 by shRNA (Fig. 4i) and observed a significant decrease in expression levels of IL-1 β (LPS group: 2.39 ± 0.27 ; LPS/F7i 2 group: 1.32 ± 0.06 ; $p < 0.01$, vs. LPS group; $n = 4$; LPS/F5i 3 group: 1.68 ± 0.16 ; $p < 0.05$, vs. LPS group; $F(3, 12) = 12.21$, $n = 4$) (Fig. 4j, k) and TNF- α (LPS group: 2.15 ± 0.14 ; LPS/F7i 2 group: 1.37 ± 0.07 ; $p < 0.01$, vs. LPS group; $n = 4$; LPS/F5i 3 group: 1.19 ± 0.16 ; $p < 0.01$, vs. LPS group; $F(3, 12) = 19.02$, $n = 4$) (Fig. 4j, l), in both FABP5- and FABP7-knockdown astrocytes.

Collectively, MF 6 treatment markedly decreased the number of astrocytes in the spinal cord following EAE induction, significantly inhibited proinflammatory cytokine accumulation, and reduced the astrocyte-dependent inflammatory response by inhibiting both FABP5 and FABP7.

3.4. MF 6 protects oligodendrocytes by inhibiting mitochondrial macropore formation

Previously, we have reported that FABP5 is involved in VDAC-1- and BAX-dependent macropore formation under psychosine exposure. Additionally, the inhibition of FABP5 by FABP5 inhibitors (such as MF 6) suggested potent effects on blocking mitochondrial macropore formation, thereby rescuing oligodendrocytes.[24] In the

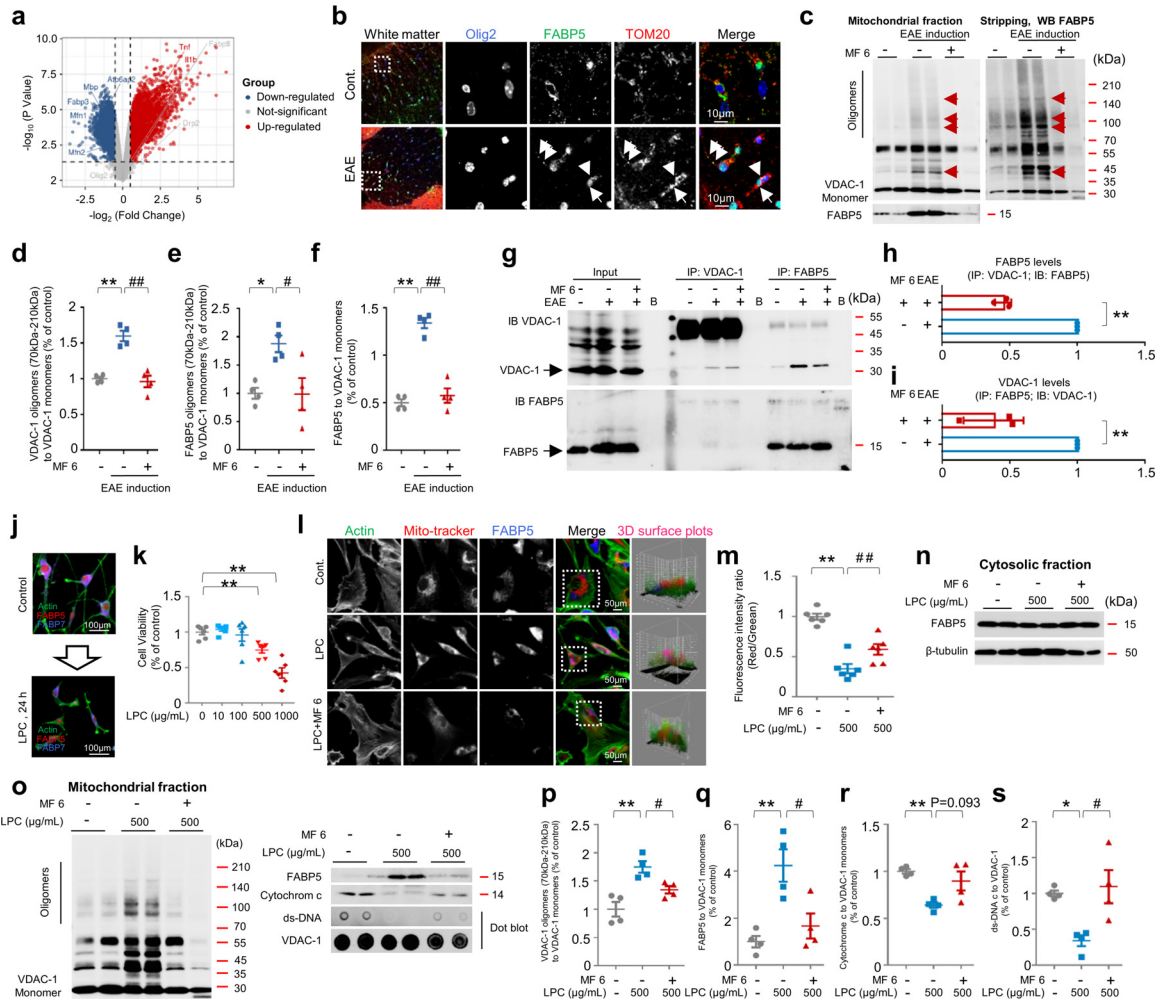


Fig. 5. MF 6 protects oligodendrocytes by improving mitochondrial function. (a) Volcano plot of the \log_2 fold change ($n=3$) on the X-axis and \log_{10} of the p -value derived using two-way ANOVA. Each point represents an individual mRNA; coloured points represent significantly changed mRNA, and grey points represent non-significant mRNA. Mitochondria-related mRNA (MFN1, MFN2, and ATP6AP2) are significantly downregulated in EAE mice. (b) Confocal microscopy of immunofluorescence staining of Olig2 (blue), FABP5 (green), TOM20 (red) in a cross-section of the spinal cord, indicating the co-localisation of FABP5 and mitochondria in oligodendrocytes of EAE mice. (c) Immunoblots and densitometry of astrocytes against antibody VDAC-1 and FABP5 in mitochondrial fraction of the spinal cord. (d-f) Quantification of (c) ($n=4$); symptomatic treatment with MF 6 (1 mg/kg) decreases the abnormally upregulated levels of VDAC-1 oligomers and FABP5 oligomers and monomers in the mitochondrial fractions of the spinal cord of EAE mice. (g) Co-immunoprecipitation of FABP5 and VDAC-1 suggests that FABP5 forms complexes with VDAC-1 in the spinal cord of EAE mice, and MF 6 markedly blocks FABP5 and VDAC-1 interaction. (h and i) Quantification of (g) ($n=3$). (j) Confocal microscopy of immunofluorescent staining with actin (green), FABP5 (red), and FABP7 (blue); KG-1C cells were treated with LPC (500 $\mu\text{g}/\text{mL}$) for 48 h. (k) Cell viability analysis of KG-1C cells using a cell counting kit assay. KG-1C cells were treated with LPC at various concentrations. (l) Confocal microscopy of immunofluorescent staining with actin (green), Mito-tracker (red), and FABP5 (blue), revealing an increased co-localisation of FABP5 and mitochondria in LPC-treated cells. Three-dimensional surface plots were measured using ImageJ software. (m) Analysis of mitochondrial membrane potential by JC-1 assay. KG-1C cells were treated with LPC (10 μM) and MF 6 (1 μM), showing a recovery in mitochondrial membrane potential in MF 6-treated cells ($n=6$). (n) Immunoblots and densitometry of the cytosolic fraction of KG-1C cells against antibody FABP5 and β -tubulin. No changes in FABP5 levels can be observed in the cytosolic fraction of LPC-treated cells. (o) Immunoblots, dot blot, and densitometry of the mitochondrial fraction of KG-1C cells against antibodies VDAC-1, FABP5, cytochrome c, and dsDNA. MF 6 (1 μM) decreases VDAC-1 oligomers and FABP5 levels in the mitochondrial fraction and blocks cytochrome c and dsDNA release from mitochondria to cytosol. (p-s) Quantification of (o) ($n=4$). Data are shown as mean \pm standard error of the mean (SEM) and were obtained using a one-way ANOVA or Kruskal-Wallis test. ** $p < 0.01$, * $p < 0.05$, and ## $p < 0.01$. Cont., control; EAE, experimental autoimmune encephalomyelitis; IP, immunoprecipitation; IB, immunoblotting; FABP5, fatty acid protein 5; FABP7, fatty acid protein 7; VDAC-1, voltage-dependent anion channel; LPC, lysophosphatidylcholine.

present study, DNA microarray analysis revealed that mitochondria-related genes, such as mitochondrial fusion proteins 1 and 2 (*MFN1*, 2) and *ATP6AP2*, were downregulated in the spinal cord of EAE mice (Fig. 5a) (original data are from Gene Expression Omnibus [GSE60847]). Furthermore, using a spinal cord slice, FABP5 was double-stained with the mitochondrial outer membrane protein TOM20. We observed that FABP5 co-localised with TOM20 in oligodendrocytes of EAE mice (Fig. 5b). To further determine whether VDAC-1-dependent macropore formation is stimulated in EAE mice, we blotted mitochondrial fractions with VDAC-1 antibody and detected elevated VDAC-1 oligomer levels in the spinal cord of EAE mice (VDAC-1 oligomer levels in the control group: 1.00 ± 0.03 ; EAE group: 1.59 ± 0.07 ; $p < 0.01$, vs. control group; $n = 4$) (Fig. 5c, d), suggesting accelerated mitochondrial macropore formation. On blotting the same

membrane with FABP5 antibody after stripping, we detected increased levels of FABP5 in both oligomers (FABP5 oligomer levels in the control group: 1.00 ± 0.09 ; EAE group: 1.88 ± 0.15 ; $p < 0.05$, vs. control group; $n = 4$) (Fig. 5c, e) and monomers (FABP5 monomer levels in the control group: 1.00 ± 0.07 ; EAE group: 2.68 ± 0.11 ; $p < 0.01$, vs. control group; $n = 4$) (Fig. 5c, f), suggesting that FABP5 is also associated with VDAC-1 oligomerisation in EAE mice. In MF 6-treated mice, we observed reduced levels of both VDAC-1 (VDAC-1 oligomer levels in EAE+MF 6 group: 0.96 ± 0.08 ; $p < 0.01$, vs. EAE group; $F(2, 9) = 30.08$, $n = 4$) (Fig. 5d) and FABP5 oligomers (FABP5 oligomer levels in EAE+MF 6 group: 0.99 ± 0.28 ; $p < 0.05$, vs. EAE group; $F(2, 9) = 6.99$, $n = 4$) (Fig. 5e) and monomers (FABP5 monomer levels in EAE+MF 6 group: 1.15 ± 0.15 ; $p < 0.01$, vs. EAE group; $F(2, 9) = 64.45$, $n = 4$) (Fig. 5f) in the mitochondria; consistently, the

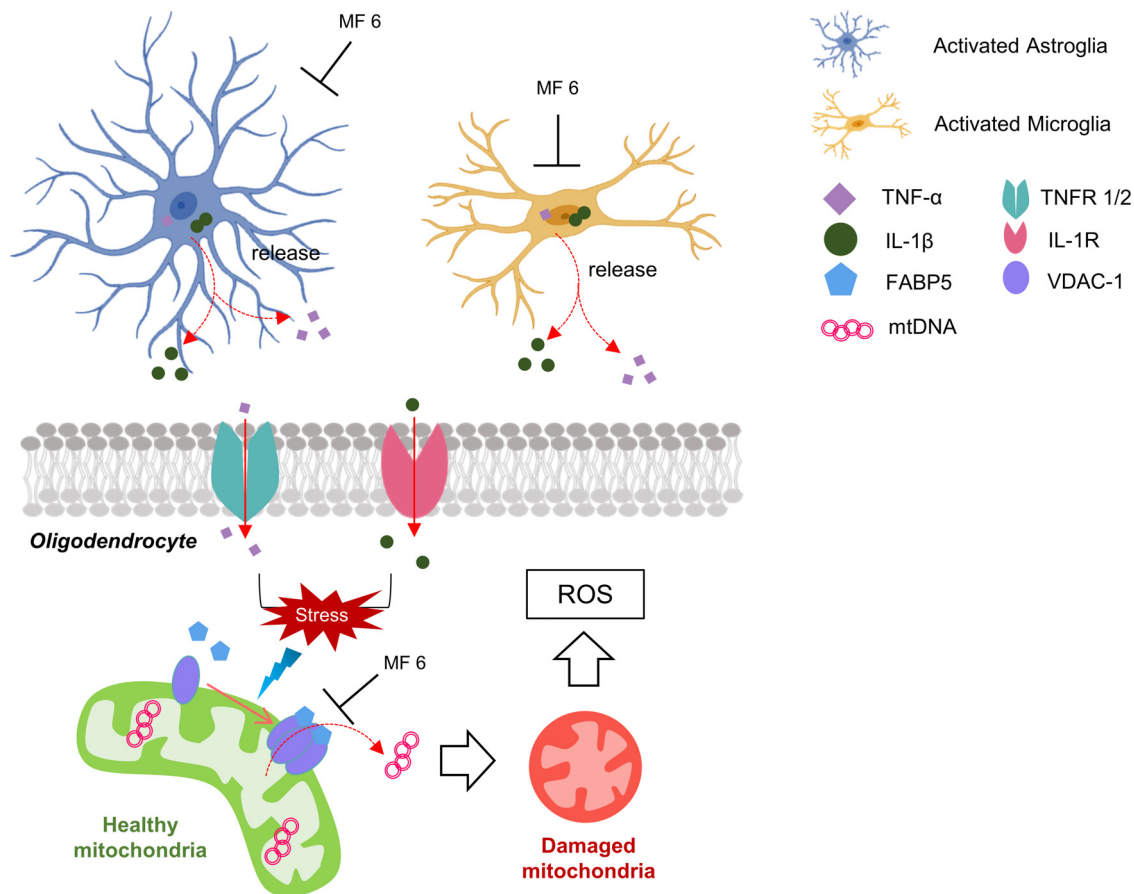


Fig. 6. Schematic representation of pathways underlying MF 6-mediated therapy in EAE. MF 6 inhibits inflammatory response by inhibiting TNF- α and IL-1 β accumulation and release in astrocytes and microglia. On the other hand, MF 6 also reduces mitochondria macropore formation, thereby reducing ROS levels, and improves oligodendrocyte survival. Overall, MF 6 is one potential therapeutic approach for MS therapy via the two pathways. EAE, experimental autoimmune encephalomyelitis; IL-1 β , interleukin-1 β ; TNF- α , tumour necrosis factor- α ; ROS, reactive oxygen species.

VDAC-1 and FABP5 interactions were significantly disrupted by MF 6 (FABP5 levels in EAE+MF 6 group: 0.45 ± 0.03 ; $p < 0.01$, vs. EAE group, $n = 3$; VDAC-1 levels in EAE+MF 6 group: 0.38 ± 0.13 ; $p < 0.01$, vs. EAE group, $n = 3$) (Fig. 5g, h, i). This suggested that MF 6 blocked VDAC-1 and FABP5 interactions, thereby inhibiting VDAC-1 oligomerisation.

To further verify our hypothesis *in vitro*, we treated KG-1C cells with LPC to trigger demyelination and loss of oligodendrocytes in cellular models of MS (Fig. 5j) [37]. As LPC induced significant cell death at $1000 \mu\text{g/mL}$ (cell viability in the LPC [$1000 \mu\text{g/mL}$] group: 0.42 ± 0.07 ; $p < 0.01$, vs. control group; $F(4, 25) = 19.75$, $n = 6$) (Fig. 5k), we selected a medium toxic concentration ($500 \mu\text{g/mL}$) for cell treatment. We observed that FABP5 was localised in the mitochondria of cells treated with LPC ($500 \mu\text{g/mL}$) (Fig. 5l), triggering a significant loss of mitochondrial membrane potential (Fig. 5m). However, MF 6 ($1 \mu\text{M}$) treatment significantly blocked the abnormal accumulation of FABP5 in the mitochondria (Fig. 5l) and improved mitochondrial membrane potential (LPC [$500 \mu\text{g/mL}$] group: 0.35 ± 0.06 ; LPC [$500 \mu\text{g/mL}$]+MF 6 group: 0.59 ± 0.07 ; $p < 0.01$, vs. LPC [$500 \mu\text{g/mL}$] group; $F(2, 15) = 34.53$, $n = 6$) (Fig. 5m). Although no changes in FABP5 were observed in the cytosolic fraction (Fig. 5n), both VDAC-1 oligomers (LPC [$500 \mu\text{g/mL}$] group: 1.75 ± 0.10 ; $p < 0.01$, vs. control group, $n = 4$) (Fig. 5o, p) and FABP5 (LPC [$500 \mu\text{g/mL}$] group: 4.25 ± 0.69 ; $p < 0.01$; control group, $n = 4$) (Fig. 5o, q) were significantly elevated in the mitochondrial fraction of LPC-treated cells, suggesting accelerated mitochondrial micropore formation. In addition, we observed an obvious release of cytochrome c (LPC [$500 \mu\text{g/mL}$] group: 0.64 ± 0.03 ; $p = 0.0723$, vs. control group, $n = 4$) (Fig. 5o, r) and mitochondrial DNA (mtDNA) (LPC [$500 \mu\text{g/mL}$] group: 0.34 ± 0.08 ;

$p < 0.05$, vs. control group, $n = 4$) (Fig. 5o, s) from the mitochondria. *In vitro*, MF 6 significantly decreased VDAC-1 oligomer formation (LPC [$500 \mu\text{g/mL}$]+MF 6 group: 1.35 ± 0.07 ; $p < 0.05$, vs. LPC [$500 \mu\text{g/mL}$] group; $F(2, 9) = 13.51$, $n = 4$) (Fig. 5p), accumulation of FABP5 (LPC [$500 \mu\text{g/mL}$]+MF 6 group: 1.67 ± 0.53 ; $p < 0.05$, vs. LPC [$500 \mu\text{g/mL}$] group; $F(2, 9) = 10.87$, $n = 4$) (Fig. 5q) and mtDNA (LPC [$500 \mu\text{g/mL}$]+MF 6 group: 1.09 ± 0.23 ; $p < 0.05$, vs. LPC [$500 \mu\text{g/mL}$] group; $F(2, 9) = 8.22$, $n = 4$) (Fig. 5s), as well as reduced the release of cytochrome c, although not significantly but obviously (LPC [$500 \mu\text{g/mL}$]+MF 6 group: 0.897 ± 0.10 ; $p = 0.093$, vs. LPC [$500 \mu\text{g/mL}$] group; $n = 4$) (Fig. 5r), from the mitochondria to the cytoplasm.

Collectively, FABP5 was involved in the mitochondrial damage of oligodendrocytes in both EAE mice and the cellular MS model. Inhibition of FABP5 by MF 6 suggests potent effects on macropore inhibition, thereby rescuing oligodendrocytes.

Figure 6

4. Discussion

MS is an autoimmune disease that targets the myelin of the central and peripheral nervous systems. MS is potentially associated with auto-reactive CD4⁺ T cells, which are activated in the periphery and cross the blood-brain barrier (BBB) to reach the CNS. This migration triggers an inflammatory reaction, including the recruitment of other leucocytes, such as B cells and macrophages [38]. Additionally, recent studies have indicated an important role of local microglia [39,40] and astrocytes, [41,42] which promote inflammation, demyelination, and neurodegeneration and critically contribute to the

Table 1
Key resources of antibodies.

Designation	Source	Identifiers	Dilution ratio	RRID
Caveolin-1	BD Transduction Laboratories	610406	1:500	AB_2314110
Iba-1	Fujifilm	016-20001	1:1000	AB_839506
4-HNE	JalCA	MHN-100P	1:1000	AB_1106813
TNF- α	Abcam	ab92324	1:500	AB_10561788
IL-1 β	Abcam	ab9722	1:1000	AB_308765
MBP	Abcam	ab7349	1:500	AB_305869
FABP5	R&D Systems	AF3077	1:200	AB_2100340
FABP7	R&D Systems	AF3166	1:200	AB_2100475
VDAC-1	CST	4866	1:500	AB_2272627This is not a pattern of 'rridsoftware' external object linking.
β -tubulin	Sigma-Aldrich	T0198	1:4000	AB_477556
Olig2	Sigma-Aldrich	MABN50	1:500	AB_10807410
dsDNA	Abcam	ab27156	1:1000	AB_470907
Cytochrome C	CST	4272	1:1000	AB_2090454
TOM20	Santa Cruz	sc-11415	1:500	AB_2207533
Anti-mouse IgG (H&L)	SouthernBiotech	1031-05	1:5000	AB_2794307
Anti-rabbit IgG (H&L)	SouthernBiotech	4050-05	1:5000	AB_2795955
Anti-goat IgG (H&L)	Rockland Immunochemicals	605-4302	1:5000	AB_219485
Alexa 405-labelled anti-mouse IgG	Thermo Fisher Scientific	A-31553	1:500	AB_221604
Alexa 488-labelled anti-goat IgG	Thermo Fisher Scientific	A-11055	1:500	AB_2534102
Alexa 594-labelled anti-mouse IgG	Thermo Fisher Scientific	A-21203	1:500	AB_141633
Alexa 594-labelled anti-rabbit IgG	Thermo Fisher Scientific	A-21207	1:500	AB_141637

Iba-1, ionised calcium-binding adaptor protein-1; 4-HNE, 4-hydroxynonal; IL-1 β , interleukin-1 β ; TNF- α , tumour necrosis factor- α ; MBP, myelin basic protein; FABP5, fatty acid protein 5; FABP7, fatty acid protein 7. This is not a pattern of 'rridsoftware' external object linking.

development of MS injuries [43,44]. Microglial activation in the early stages of MS results in increased microglial proliferation in response to neuronal insults. In the present study, we detected an increased number of Iba-1-positive cells in the spinal cord of EAE mice. Moreover, abnormal accumulation of activated microglia clusters can be observed in the white matter of patients with MS and are associated with degenerating axons, stressed oligodendrocytes, or deposits of activated products in the complement pathway [45,46]. However, in addition to leucocytes, including T cells, B cells, and macrophages, stimulated microglia and astrocytes also secrete inflammatory cytokines such as TNF- α , IL-1 β , and IL-6, [41] known to be involved in the secondary oxidative stress targeting oligodendrocytes as an internal mechanism for MS pathology.

Table 1

In an attempt to target the inflammatory response, a previous study has investigated the effects of FABP5 inhibitors, which regulate the functions of antigen-presenting cells and T cells and inhibit lymphocyte migration and pathogenic functions [17]. In the present study, MF 6 significantly improved the neurological scores of EAE mice, as well as reversed the increased oxidation and caveolin-1 levels, suggesting a protective effect on the BBB [47]. We observed that MF 6 decreased cytokine levels in the spinal cord, which might mediate FABP5 and FABP7 inhibition. Accordingly, the attenuated inflammatory responses in the CNS may be related to decreased levels of oxidative injury [48]. Consistently, MF 6 significantly decreased oxidative stress levels in oligodendrocytes and neurons.

In a previous study, FABP5 deficiency was shown to inhibit the proinflammatory T cell-mediated promotion of macrophages and dendritic cells [16] via enhanced PPAR γ activity [49-51]. FABP7 deficiency is also involved in the loss function of lipid rafts and significantly decreases TNF- α production [52]. Although we could not clarify the detailed underlying mechanism, both FABP5 and FABP7 deficiency, induced by shRNA, regulated TNF- α and IL-1 β secretion in primary astrocyte cultures. Taken together, MF 6 elicits inhibitory effects on both cytokine production and secretion via FABP5 and FABP7 inhibition.

We have recently reported that FABP5 forms complexes with VDAC-1 protein and induces VDAC-1 oligomer-dependent mitochondrial macropore formation. Furthermore, inhibition of FABP5 by MF 6 improved mitochondrial function and rescued oligodendrocytes from psychosine-mediated toxicity [24]. Thus, we postulated that FABP5 also mediates mitochondrial dysfunction in EAE mice. MF 6 protected oligodendrocytes from this pathway via FABP5 inhibition. Moreover, we observed impaired mitochondrial functions in both EAE- and LPC-stimulated KG-1C cells. As expected, MF 6 significantly disrupted FABP5 and VDAC-1 complexes, thereby blocking mitochondrial macropore formation. This finding might explain the inhibition of mtDNA and cytochrome c release and the rescue of mitochondria.

Previous studies have revealed that FABP5 upregulation exacerbates the development of EAE, a mouse model of human MS [16]. Additionally, FABP5, which is expressed in dendritic cells and macrophages, promotes the generation of inflammatory cytokines such as TNF α and IL-1 β [16]. These elevated levels were attenuated following MF6 administration. Furthermore, during early MS progression, astrocytes exhibit morphological and biochemical alterations, leading to astrogliosis [53]. Notably, FABP7 expressed in the astrocyte lineage was considerably upregulated by activated astrocytes during the early progression of MS [54-56]. In the present study, MF 6 improved neurological behaviours and reduced the expression of inflammatory factors following both prophylactic and symptomatic treatment regimens. This may indicate a potential effect of MF 6 in treating relapsing-remitting MS. In a previous study, MF 6 administration did not induce toxicity at high doses [17]. However, the secondary target of FABP5 inhibitors remains unclear. PPAR γ may also exert protective effects in ameliorating MS [17]. Moreover, in our previous study, MF 6 was shown to reduce cell proliferation in U251 cells, [22] which may be associated with the FABP7 inhibition. Currently, FABP inhibition therapy remains in the preclinical stage, and potential adverse reactions following clinical application remain uncertain. However, we have initiated a toxicological evaluation of FABP inhibitors, including MF 6. We hope that MF 6 and other efficient ligands can be employed for MS therapy in the future.

In the present study, FABP5 and FABP7 inhibitor, MF 6, improved the severity of EAE and attenuated oxidative levels and the inflammatory response, indicating close associations between these factors and EAE progression. However, it is difficult to confirm whether these factors induce or result in MS progression based on the present findings. We observed that the inhibition of FABP5 and FABP7 by MF 6 decreased both the immune response and oxidative stress, thereby rescuing oligodendrocytes and improving EAE progression. Although we were unable to determine which cytokines are released from T cells, dendritic cells, astrocytes, and microglia and whether the cytokines stimulate oxidative stress in the acceptor cells such as neurons and oligodendrocytes, it will be of considerable interest to address these issues in future investigations.

As the therapeutic effect of FABP5 inhibitors has been previously defined by other groups,^[17] in the present study, we focused on the local activation of astrocytes, microglia, and oligodendrocytes in the spinal cord. In summary, MF 6 attenuated the inflammatory response of activated microglia and astrocytes by inhibiting FABP5 and FABP7. Furthermore, MF 6 improved the survival of oligodendrocytes by disrupting FABP5/VDAC-1-dependent mitochondrial macropore formation, thus rescuing mitochondria. Importantly, MF 6 reduced clinical symptoms of EAE following both the prophylactic and symptomatic treatments. Thus, MF 6 is a novel and potential therapeutic approach for MS.

Declaration of Competing Interest

The authors have declared that no conflict of interest exists.

Contributors

A. Cheng: Data acquisition and original draft writing
W. Jia: Data acquisition and design of the methodology
I. Kawahata: Data acquisition
K. Fukunaga: Supervision, project administration, funding, and reviewing and editing the manuscript.

All authors critically reviewed the manuscript and approved the final version of the manuscript. A. Cheng and K. Fukunaga verified the data and had final responsibility for the decision to submit for publication.

Acknowledgements

We thank the Uehara Memorial Foundation and the Japan Agency for Medical Research and Development (AMED) (grant numbers 20dm0107071) for the financial support provided.

Data Sharing Statement

The data supporting the findings of this study are available in the article and/or supplementary materials. The data in Fig. 5a were based on publicly available data from the Gene Expression Omnibus (GEO; <https://www.ncbi.nlm.nih.gov/geo/query/acc.cgi?acc=GSE60847>). Readers are welcome to contact the corresponding author for the raw data used in this work.

Supplementary materials

Supplementary material associated with this article can be found, in the online version, at doi:10.1016/j.ebiom.2021.103582.

References

[1] Kaminska J, Koper OM, Piechal K, Kemonia H. Multiple sclerosis - etiology and diagnostic potential. *Postepy Hig Med Dosw (Online)* 2017;71(0):551–63.

- [2] McFarland HF, Martin R. Multiple sclerosis: a complicated picture of autoimmunity. *Nat Immunol* 2007;8(9):913–9.
- [3] Hart FM, Bainbridge J. Current and emerging treatment of multiple sclerosis. *Am J Manag Care* 2016;22(6 Suppl):s159–70.
- [4] Brunkhorst R, Vutukuri R, Pfeilschifter W. Fingolimod for the treatment of neurological diseases—state of play and future perspectives. *Front Cell Neurosci* 2014;8:283.
- [5] Nazareth T, Friedman HS, Navaratnam P, et al. Persistency, medication prescribing patterns, and medical resource use associated with multiple sclerosis patients receiving oral disease-modifying therapies: a retrospective medical record review. *BMC Neurol* 2016; 16(1):187.
- [6] Veerkamp JH, Peeters RA, Maatman RG. Structural and functional features of different types of cytoplasmic fatty acid-binding proteins. *Biochim Biophys Acta* 1991;1081(1):1–24.
- [7] Coe NR, Bernlohr DA. Physiological properties and functions of intracellular fatty acid-binding proteins. *Biochim Biophys Acta* 1998;1391(3):287–306.
- [8] Spener F, Borchers T, Mukherjea M. On the role of fatty acid binding proteins in fatty acid transport and metabolism. *FEBS Lett* 1989;244(1):1–5.
- [9] Zhang Y, Sun Y, Rao E, et al. Fatty acid-binding protein E-FABP restricts tumor growth by promoting IFN- β responses in tumor-associated macrophages. *Cancer Res* 2014;74(11):2986–98.
- [10] Makowski L, Brittingham KC, Reynolds JM, Suttles J, Hotamisligil GS. The fatty acid-binding protein, aP2, coordinates macrophage cholesterol trafficking and inflammatory activity. Macrophage expression of aP2 impacts peroxisome proliferator-activated receptor gamma and I κ B kinase activities. *J Biol Chem* 2005;280(13):12888–95.
- [11] Matsuo K, Cheng A, Yabuki Y, Takahata I, Miyachi H, Fukunaga K. Inhibition of MPTP-induced α -synuclein oligomerization by fatty acid-binding protein 3 ligand in MPTP-treated mice. *Neuropharmacology* 2019; 150:164–74.
- [12] Wang Y, Shinoda Y, Cheng A, Kawahata I, Fukunaga K. Epidermal Fatty Acid-Binding Protein 5 (FABP5) Involvement in Alpha-Synuclein-Induced Mitochondrial Injury under Oxidative Stress. *Biomedicines* 2021;9(2):110.
- [13] Cheng A, Jia W, Kawahata I, Fukunaga K. Impact of Fatty Acid-Binding Proteins in α -Synuclein-Induced Mitochondrial Injury in Synucleinopathy. *Biomedicines* 2021;9(5):560.
- [14] Jia W, Wilar G, Kawahata I, Cheng A, Fukunaga K. Impaired Acquisition of Nicotine-Induced Conditioned Place Preference in Fatty Acid-Binding Protein 3 Null Mice. *Mol Neurobiol* 2021;58(5):2030–45.
- [15] Li B, Reynolds JM, Stout RD, Bernlohr DA, Suttles J. Regulation of Th17 differentiation by epidermal fatty acid-binding protein. *J Immunol* 2009;182(12):7625–33.
- [16] Reynolds JM, Liu Q, Brittingham KC, et al. Deficiency of fatty acid-binding proteins in mice confers protection from development of experimental autoimmune encephalomyelitis. *J Immunol* 2007;179(1):313–21.
- [17] Rao E, Singh P, Li Y, et al. Targeting epidermal fatty acid binding protein for treatment of experimental autoimmune encephalomyelitis. *BMC Immunol* 2015;16:28.
- [18] Clemente D, Ortega MC, Melero-Jerez C, de Castro F. The effect of glia-glia interactions on oligodendrocyte precursor cell biology during development and in demyelinating diseases. *Front Cell Neurosci* 2013; 7:268.
- [19] Domingues HS, Portugal CC, Socodato R, Relvas JB. Oligodendrocyte, Astrocyte, and Microglia Crosstalk in Myelin Development, Damage, and Repair. *Front Cell Dev Biol* 2016;4:71.
- [20] Kamizato K, Sato S, Shil SK, et al. The role of fatty acid binding protein 7 in spinal cord astrocytes in a mouse model of experimental autoimmune encephalomyelitis. *Neuroscience* 2019; 409:120–9.
- [21] Shinoda Y, Wang Y, Yamamoto T, Miyachi H, Fukunaga K. Analysis of binding affinity and docking of novel fatty acid-binding protein (FABP) ligands. *J Pharmacol Sci* 2020;143(4):264–71.
- [22] Cheng A, Wang Y-f, Shinoda Y, et al. Fatty acid-binding protein 7 triggers α -synuclein oligomerization in glial cells and oligodendrocytes associated with oxidative stress. *Acta Pharmacol Sin* 2021.
- [23] Cheng A, Shinoda Y, Yamamoto T, Miyachi H, Fukunaga K. Development of FABP3 ligands that inhibit arachidonic acid-induced alpha-synuclein oligomerization. *Brain Res* 2019;1707:190–7.
- [24] Cheng A, Kawahata I, Fukunaga K. Fatty Acid Binding Protein 5 Mediates Cell Death by Psychosine Exposure through Mitochondrial Macropores Formation in Oligodendrocytes. *Biomedicines* 2020;8(12).
- [25] Guo Q, Kawahata I, Degawa T, et al. Fatty Acid-Binding Proteins Aggravate Cerebral Ischemia-Reperfusion Injury in Mice. *Biomedicines* 2021;9(5).
- [26] Terry RL, Ifergan I, Miller SD. Experimental Autoimmune Encephalomyelitis in Mice. *Methods Mol Biol* 2016;1304:145–60.
- [27] Martins-Branco D, Esteves AR, Santos D, et al. Ubiquitin proteasome system in Parkinson's disease: a keeper or a witness? *Exp Neurol* 2012;238(2):89–99.
- [28] Sun M, Shinoda Y, Fukunaga K. KY-226 Protects Blood-brain Barrier Function Through the Akt/FoxO1 Signaling Pathway in Brain Ischemia. *Neuroscience* 2019; 399:89–102.
- [29] Ljubisavljevic S, Stojanovic I, Pavlovic D, Sokolovic D, Stevanovic I. Aminoguanidine and N-acetyl-cysteine suppress oxidative and nitrosative stress in EAE rat brains. *Redox Rep* 2011;16(4):166–72.
- [30] Dunham J, Bauer J, Campbell GR, et al. Oxidative Injury and Iron Redistribution Are Pathological Hallmarks of Marmoset Experimental Autoimmune Encephalomyelitis. *J Neuropathol Exp Neurol* 2017;76(6):467–78.
- [31] Yuan D, Cheng A, Kawahata I, Izumi H, Xu J, Fukunaga K. Single Administration of the T-Type Calcium Channel Enhancer SAK3 Reduces Oxidative Stress and Improves Cognition in Olfactory Bulbectomized Mice. *Int J Mol Sci* 2021;22(2).

- [32] Jia Z, Zhu H, Li J, Wang X, Misra H, Li Y. Oxidative stress in spinal cord injury and antioxidant-based intervention. *Spinal Cord* 2012;50(4):264–74.
- [33] Cao Y, Goods BA, Raddassi K, et al. Functional inflammatory profiles distinguish myelin-reactive T cells from patients with multiple sclerosis. *Sci Transl Med* 2015;7(287) 287ra74.
- [34] Olsson T, Zhi WW, Höjeberg B, et al. Autoreactive T lymphocytes in multiple sclerosis determined by antigen-induced secretion of interferon-gamma. *J Clin Invest* 1990;86(3):981–5.
- [35] Rothhammer V, Borucki DM, Tjon EC, et al. Microglial control of astrocytes in response to microbial metabolites. *Nature* 2018; 557(7707):724–8.
- [36] Rizzo FR, Musella A, De Vito F, et al. Tumor Necrosis Factor and Interleukin-1beta Modulate Synaptic Plasticity during Neuroinflammation. *Neural Plast* 2018;2018:8430123.
- [37] Kipp M, van der Star B, Vogel DY, et al. Experimental in vivo and in vitro models of multiple sclerosis: EAE and beyond. *Multiple Scler Relat Disord* 2012; 1(1):15–28.
- [38] Ruiz F, Vigne S, Pot C. Resolution of inflammation during multiple sclerosis. *Semin Immunopathol* 2019;41(6):711–26.
- [39] Voet S, Prinz M, van Loo G. Microglia in Central Nervous System Inflammation and Multiple Sclerosis Pathology. *Trends Mol Med* 2019;25(2):112–23.
- [40] Chu F, Shi M, Zheng C, et al. The roles of macrophages and microglia in multiple sclerosis and experimental autoimmune encephalomyelitis. *J Neuroimmunol* 2018;318:1–7.
- [41] Ponath G, Park C, Pitt D. The Role of Astrocytes in Multiple Sclerosis. *Front Immunol* 2018;9:217.
- [42] Allnoch L, Baumgärtner W, Hansmann F. Impact of Astrocyte Depletion upon Inflammation and Demyelination in a Murine Animal Model of Multiple Sclerosis. *Int J Mol Sci* 2019;20(16).
- [43] Frischer JM, Bramow S, Dal-Bianco A, et al. The relation between inflammation and neurodegeneration in multiple sclerosis brains. *Brain: a journal of neurology* 2009;132(Pt 5):1175–89.
- [44] Dendrou CA, Fugger L, Friese MA. Immunopathology of multiple sclerosis. *Nat Rev Immunol* 2015;15(9):545–58.
- [45] Ramaglia V, Hughes TR, Donev RM, et al. C3-dependent mechanism of microglial priming relevant to multiple sclerosis. *PNAS* 2012;109(3):965–70.
- [46] Singh S, Metz I, Amor S, van der Valk P, Stadelmann C, Brück W. Microglial nodules in early multiple sclerosis white matter are associated with degenerating axons. *Acta Neuropathol (Berl)* 2013;125(4):595–608.
- [47] Shin T, Kim H, Jin JK, et al. Expression of caveolin-1, -2, and -3 in the spinal cords of Lewis rats with experimental autoimmune encephalomyelitis. *J Neuroimmunol* 2005;165(1–2):11–20.
- [48] Lassmann H, van Horssen J. Oxidative stress and its impact on neurons and glia in multiple sclerosis lesions. *Biochim Biophys Acta* 2016;1862(3):506–10.
- [49] Diab A, Deng C, Smith JD, et al. Peroxisome proliferator-activated receptor-gamma agonist 15-deoxy-Delta(12,14)-prostaglandin J(2) ameliorates experimental autoimmune encephalomyelitis. *J Immunol* 2002;168(5):2508–15.
- [50] Diab A, Hussain RZ, Lovett-Racke AE, Chavis JA, Drew PD, Racke MK. Ligands for the peroxisome proliferator-activated receptor-gamma and the retinoid X receptor exert additive anti-inflammatory effects on experimental autoimmune encephalomyelitis. *J Neuroimmunol* 2004;148(1–2):116–26.
- [51] Lovett-Racke AE, Hussain RZ, Northrop S, et al. Peroxisome proliferator-activated receptor alpha agonists as therapy for autoimmune disease. *J Immunol* 2004;172(9):5790–8.
- [52] Kagawa Y, Yasumoto Y, Sharifi K, et al. Fatty acid-binding protein 7 regulates function of caveolae in astrocytes through expression of caveolin-1. *Glia* 2015; 63(5):780–94.
- [53] Williams A, Piaton G, Lubetzki C. Astrocytes—friends or foes in multiple sclerosis? *Glia* 2007; 55(13):1300–12.
- [54] Mita R, Coles JE, Glubrecht DD, Sung R, Sun X, Godbout R. B-FABP-expressing radial glial cells: the malignant glioma cell of origin? *Neoplasia* 2007; 9(9):734–44.
- [55] Bannerman P, Hahn A, Soulika A, Gallo V, Pleasure D. Astrogliosis in EAE spinal cord: derivation from radial glia, and relationships to oligodendroglia. *Glia* 2007; 55(1):57–64.
- [56] Kipp M, Gingele S, Pott F, et al. BLBP-expression in astrocytes during experimental demyelination and in human multiple sclerosis lesions. *Brain Behav Immun* 2011;25(8):1554–68.